Acta Crystallographica Section D
Biological Crystallography
ISSN 0907-4449

Crystallization and preliminary X-ray analysis of tetracenomycin A2 oxygenase: a flavoprotein hydroxylase involved in polyketide biosynthesis

John Beynon,[a] Elpidio R. Rafanan Jr,[a] Ben Shen[a] and Andrew J. Fisher[a,b]*

[a]Department of Chemistry, University of California, One Shields Avenue, Davis, CA 95616, USA, and [b]Section of Molecular and Cellular Biology, University of California, One Shields Avenue, Davis, CA 95616, USA

Correspondence e-mail: fisher@chem.ucdavis.edu

Received 12 June 2000
Accepted 13 September 2000

The *tcm* operon in *Streptomyces glaucescens* encodes a group of enzymes involved in the synthesis of the polyketide tetracenomycin (Tcm) C that exhibits both antitumor and antibiotic activities. Here, the crystallization and preliminary data characterization of the *tcmG* gene product, Tcm A2 oxygenase, which catalyzes the triple hydroxylation of Tcm A2 to form Tcm C, are reported. Tcm A2 oxygenase crystallizes in two different space groups, both with six monomers per asymmetric unit, resulting in large unit-cell parameters. Synchrotron data have been collected from both the hexagonal and tetragonal crystal forms to 4.5 and 4.2 Å, respectively. The self-rotation function searches in both space groups suggest the monomers assemble into a complex with D_3 symmetry.

1. Introduction

Polyketide biosynthesis is responsible for a large number of biologically active molecules. In many cases, the activities of these natural products result from additions or modifications of functional groups after the carbon skeleton has been synthesized. Tetracenomycin (Tcm) A2 oxygenase, the product of *tcmG* identified within the *tcm* biosynthetic gene cluster from *S. glaucescens* (Decker *et al.*, 1993), catalyzes the triple hydroxylation of Tcm A2 to form Tcm C (Shen & Hutchinson, 1994). Tcm C, first isolated in 1979, has been shown to possess antibacterial and antitumor activities (Egert *et al.*, 1992; Weber *et al.*, 1979).

Tcm A2 oxygenase displays limited sequence homology to other aromatic hydroxylases whose structures have been determined, such as *p*-hydroxybenzoate hydroxylase (PHBH, 27.4% identity; Schreuder *et al.*, 1988) and phenol hydroxylase (PHHY, 25.5% identity; Enroth *et al.*, 1998); all three hydroxylases contain the flavin cofactor FAD. PHBH and PHHY catalyze the introduction of one hydroxyl, from molecular oxygen, to an aromatic ring, requiring one molar equivalent of NADPH as an electron donor. In contrast, Tcm A2 oxygenase catalyzes the stereospecific introduction of three hydroxyl groups with the concurrent oxidation of an existing hydroxyl group to a carbonyl group, requiring two molar equivalents of NADPH as an electron donor. Furthermore, $^{18}O_2$-feeding experiments showed that two of the three new hydroxyl groups originate from molecular oxygen, while the third is derived from water (Udvarnoki *et al.*, 1995). These results suggest a mechanistic analogy among Tcm A2 oxygenase, the vitamin K dependent γ-glutamyl carboxylase (Dowd *et al.*, 1994) and other oxygenases catalyzing the biosynthesis of numerous epoxyquinone or epoxysemiquinone antibiotics (Gould *et al.*, 1996). The atomic resolution structure of Tcm A2 oxygenase, therefore, would provide key insight into the mechanism of these intriguing reactions. This paper presents the crystallization of Tcm A2 oxygenase, preliminary X-ray data and self-rotation searches.

2. Materials and methods

2.1. Expression and purification

Tcm A2 oxygenase was expressed in *S. lividans* containing the pWHM68 plasmid and grown in R2YENG media. Cells were harvested and treated as described previously (Shen & Hutchinson, 1994). Purification was improved by altering the chromatography as follows. Resuspended ammonium sulfate cut, 46–57%, was dialyzed against 25 m*M* Tris pH 8.0 for ion-exchange chromatography on a Q Sepharose FF column (Pharmacia, Piscataway, NJ, USA) and eluted with a 0.0–0.6 *M* NaCl gradient. Fractions with oxygenase activity were pooled and brought to 1.5 *M* ammonium sulfate by the addition of solid reagent. The solution was then loaded onto a Poros ET/M hydrophobic interaction column (PE Biosystems, Foster City, California, USA) and eluted with a 1.5–0.0 *M* ammonium sulfate gradient. Active fractions were then pooled and dialyzed against 25 m*M* Tris pH 8.0. A final anion-exchange purification was performed with Poros HQ media (PE Biosystems, Foster City, California, USA), eluted with a 0.0–0.8 *M* NaCl gradient. Fractions containing Tcm A2 oxygenase were dialyzed twice against nanopure H_2O and concentrated to 20–50 mg ml^{-1}.

Before crystallization, purity was confirmed by SDS–PAGE and activity assay.

2.2. Crystallization

Tcm A2 oxygenase crystallization was initially screened at 10 mg ml^{-1} with commercially available screens (Hampton Research, California, USA) at both 294 and 277 K using the hanging-drop method (McPherson, 1976). Condition number 21 of Crystal Screen I (30% PEG 4000, 200 m*M* sodium acetate, 100 m*M* Tris pH 8.5) produced balls of needles that were yellow in colour from the FAD cofactor present in the enzyme. Increasing the sodium acetate to 300 m*M* produced small yellow hexagonal crystals. These conditions were further improved upon by substituting sodium formate for sodium acetate. A wide range of additives were experimented with to improve crystal size. Some additives, DMSO and ethylene glycol, had a beneficial effect on the size and diffraction quality of the crystals. Others, such as ammonium acetate and ammonium formate, increased the crystal size but not the diffraction quality. The largest crystals were obtained using a 2 µl drop of protein mixed with 2 µl of well solution containing 100 m*M* Tris pH 8.5, 300 m*M* sodium formate, 30% PEG 4000 and 2% ethylene glycol. Small hexagonal crystals appeared within 2–3 d and reached maximum dimensions of 0.25 × 0.2 × 0.2 mm within 3–4 weeks.

A tetragonal crystal form of Tcm A2 oxygenase was subsequently found by increasing the sodium formate concentration to 2.0 *M*. This condition was optimized to 100 m*M* Bicine pH 9.0, 2.0 *M* sodium formate and 33% PEG 4000.

2.3. X-ray data collection and processing

Cryoprotection was accomplished by replacing the mother liquor surrounding the crystal with Paratone N and then flash-freezing in liquid nitrogen (Hope, 1990). Low-temperature data (100 K) was collected with a MAR345 detector at Stanford Synchrotron Radiation Laboratory beamline 9-1 (SSRL BL 9-1). Initial indexing and data-collection strategies were determined using the program *MOSFLM*. Once collected, the data were processed with the programs *DENZO* and *SCALEPACK* (Otwinowski & Minor, 1997). Data from the

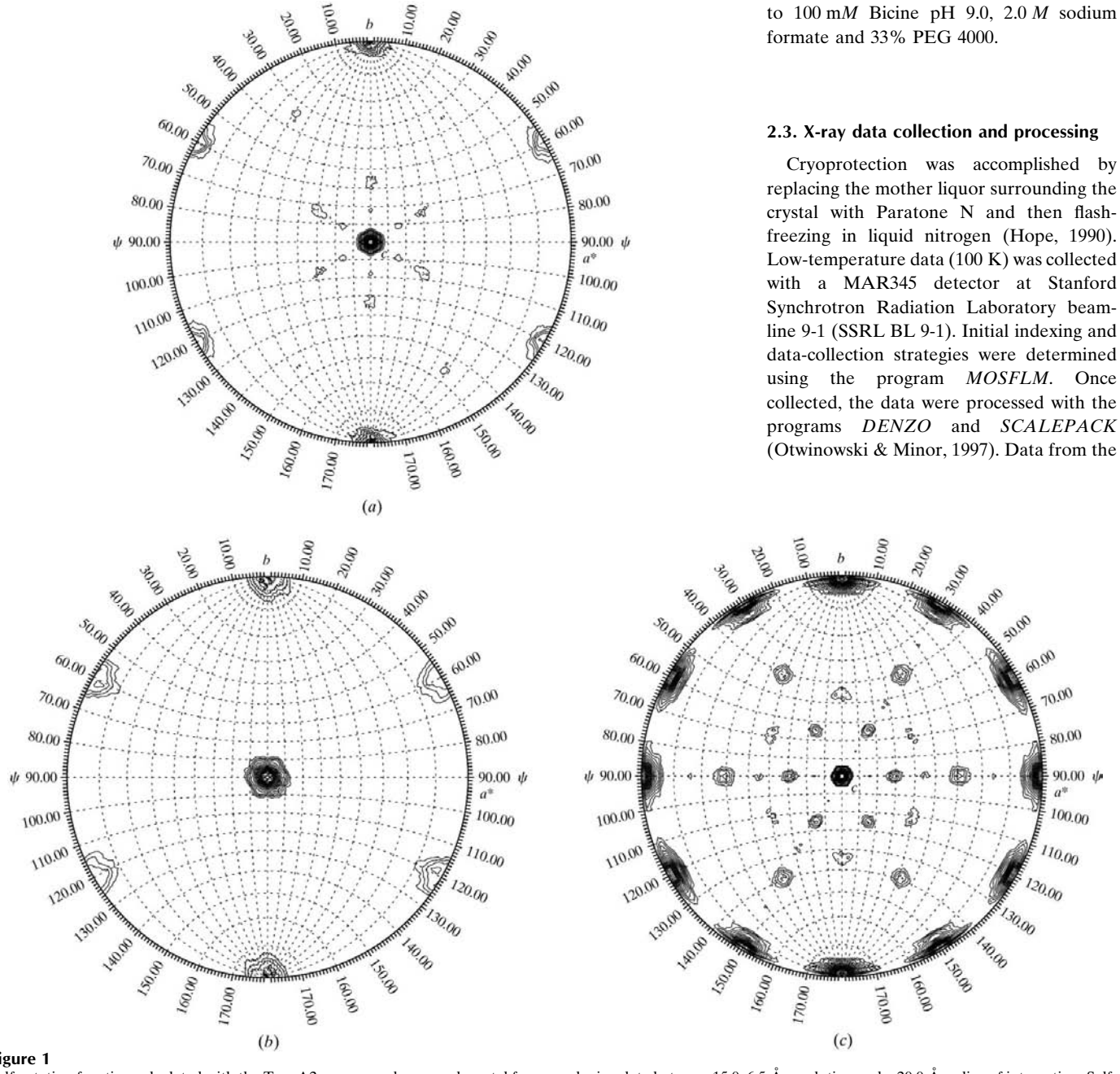

Figure 1
Self-rotation function calculated with the Tcm A2 oxygenase hexagonal crystal form employing data between 15.0–6.5 Å resolution and a 20.0 Å radius of integration. Self-rotation searches with κ angles of (*a*) $\kappa = 120$, (*b*) $\kappa = 60$ and (*c*) $\kappa = 180^\circ$ were used to identify three-, six- and twofold rotation angles, respectively, in the hexagonal crystal. The sixfold and twofold crystallographic symmetry is evident as very strong peaks in the plots. The plots were contoured starting at one standard deviation with steps of 0.5. The *GLRF* program was used to calculate and generate Figs. 1 and 2 (Tong & Rossmann, 1990).

hexagonal crystals were collected at a 500 mm crystal-to-detector distance using 0.3° oscillations. 150 exposures were collected, resulting in a 45° wedge yielding 93.5% completeness. The best data set was processed to 4.5 Å and contained 28 213 unique reflections.

The diffraction quality of the tetragonal crystal form showed improvement over the hexagonal form and a 4.2 Å data set was collected. A 90° wedge collected 98.1% of the data (33 997 unique reflections). Data from the tetragonal crystals were collected with a 450 mm crystal-to-detector distance using 0.75° oscillations. Diffraction data from this crystal form could also be indexed roughly as face-centered cubic, but data processed as *F*23 resulted in poor correlation between the predicted and observed diffraction positions and in an $R_{\rm sym}$ greater than 40%, suggesting pseudo-face-centered packing (see below). Table 1 lists data-collection statistics for both hexagonal and tetragonal crystal forms.

3. Results and discussion

3.1. Crystal forms of Tcm A2 oxygenase

The hexagonal crystal form of Tcm A2 oxygenase was shown to belong to the space group $P6_122$ (or $P6_522$), with unit-cell parameters $a = b = 237.4$, $c = 302.8$ Å. Assuming six monomers per asymmetric unit, totaling 4 320 kDa per unit cell, corresponds to a $V_{\rm M}$ of 3.42 Å^3 Da^{-1} and a solvent content of ∼64% (Matthews, 1968). While this is inconclusive, because the addition or removal of a monomer from the $V_{\rm M}$ calculation would have only a small effect, in the light of the crystallographic symmetry and self-rotation function (see below) six monomers per asymmetric unit is the most likely case. The tetragonal crystal form is in the space group $I4_122$, with unit-cell parameters $a = b = 234.8$, $c = 337.0$ Å. The tetragonal crystal form also accommodates six monomers per asymmetric unit, $V_{\rm M} = 3.23$ Å^3 Da^{-1}, ∼62% solvent content.

The cumulative intensity distributions [$N(Z)$ distributions] of both the hexagonal and tetragonal data sets were plotted using the program *TRUNCATE* (French & Wilson, 1978) from the *CCP*4 suite (Collaborative Computational Project, Number 4, 1994). The results showed little deviation between the observed and expected weak reflections, which is evidence of non-twinned single crystals (data not shown).

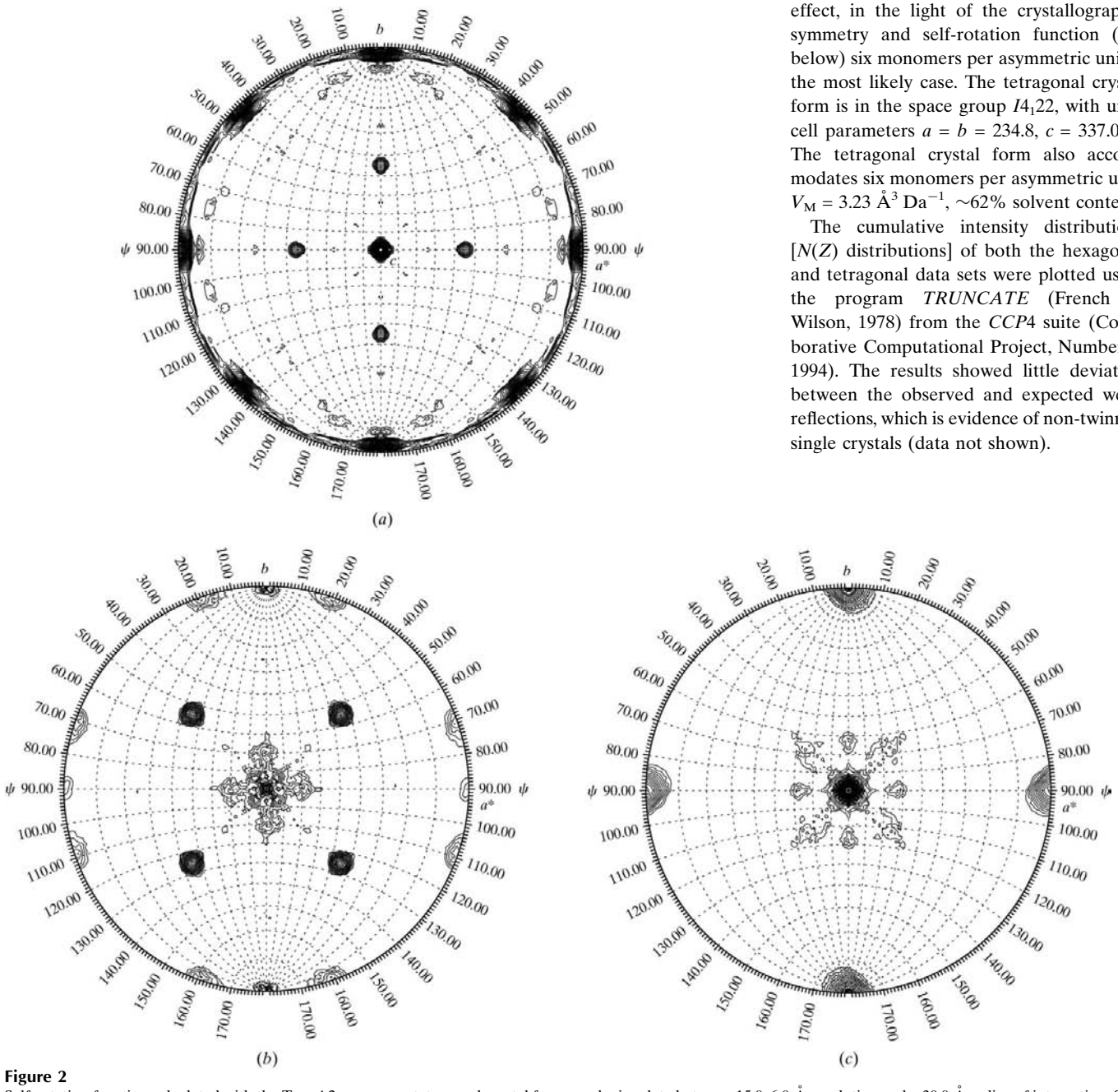

Figure 2
Self-rotation function calculated with the Tcm A2 oxygenase tetragonal crystal form employing data between 15.0–6.0 Å resolution and a 30.0 Å radius of integration. Self-rotation searches with κ angles of (*a*) $\kappa = 180$, (*b*) $\kappa = 120$ and (*c*) $\kappa = 90°$ were used to identify two-, three- and fourfold rotation angles, respectively, in the tetragonal crystal. The fourfold and twofold crystallographic symmetry is evident as very strong peaks in the plots. The presence of the non-crystallographic two- and threefold axes generates the non-crystallographic fourfold along the *a* and *b* axes as seen in (*c*). The plots were contoured starting at one standard deviation with steps of 0.5.

Table 1
Data-collection statistics.

Values in parentheses represent statistics in the highest resolution shell.

Crystal form	Hexagonal	Tetragonal
Space group	$P6_{1(5)}22$	$I4_122$
Unit-cell parameters (Å)	a = 237.4, c = 302.8	a = 234.8, c = 337.0
Wavelength (Å)	0.98	0.98
Crystal temperature (K)	100	100
Resolution (Å)	4.5	4.2
No. observed reflections	91194	139477
No. unique reflections	28213	33997
Completeness	93.5 (74.6)	98.1 (98.7)
R_{sym}†	12.9 (32.9)	12.6 (38.0)
$I/\sigma(I)$	7.5 (2.3)	10.7 (2.7)

† $R_{sym} = [\sum_h \sum_i |I_h - I_{hi}| / \sum_h \sum_i I_{hi}] \times 100$, where I_h is the mean of the I_{hi} observations of reflection h.

3.2. Self-rotation function and non-crystallographic symmetry

Using the rotation-function program *GLRF* (Tong & Rossmann, 1990), a general self-rotation function was computed with a number of κ angles (60, 90, 120 and 180°) to test for the presence of non-crystallographic two-, three-, four- and sixfold axes. A self-rotation function of the hexagonal data set with κ = 120° suggested three non-crystallographic axes in the *ab* plane: along *a* and every 60° from it (Fig. 1*a*). A function calculated with κ = 60° produced the same results, but with slightly weaker peak heights (Fig. 1*b*). If a non-crystallographic threefold is parallel to the *a* (and *b*) axis, the presence of a crystallographic twofold along these axes would generate a peak for a κ = 60° function as well. Therefore, we cannot distinguish the difference between a non-crystallographic threefold or sixfold axis parallel to the crystallographic *a* axis. A rotation function with κ = 180° showed the expected crystallographic symmetry peaks as well as the presence of non-crystallographic twofolds every 30° in planes perpendicular to each of the non-crystallographic three- or sixfolds (Fig. 1*c*). The κ = 90° calculation showed no significant symmetry (not shown).

The tetragonal data were probed in the same manner as the hexagonal data and also showed a number of non-crystallographic two-, three- and fourfolds. The rotation function calculated with κ = 180° revealed distinct non-crystallographic twofold axes 45° between the *a* and *c* axes as well as the *b* and *c* axis (Fig. 2*a*). A κ = 120° search generated four peaks 54.7° from the *a*, *b* and *c* axes (Fig. 2*b*), which would correspond to a body diagonal of a cube resulting in pseudo-face-centered cubic packing. These non-crystallographic threefolds are normal to the non-crystallographic twofold axes, generating a potential packing of monomers with D_3 point symmetry as observed in the hexagonal crystal form. This non-crystallographic 2–3 symmetry combined with the crystal 422 symmetry would generate a non-crystallographic fourfold rotational symmetry along the *a* and *b* axes, which is confirmed with a κ = 90° self-rotation search (Fig. 2*c*). A search for a non-crystallographic sixfold axis (κ = 60°) produced no significant peaks (not shown).

3.3. Cross-rotation functions

A cross-rotation function with either the PHBH or the PHHY models did not produce any significant peaks in either the hexagonal or tetragonal data sets. This indicates that these models cannot be used to solve the Tcm A2 oxygenase structure by the molecular-replacement method and that the phases must be calculated by other methods once better diffracting crystals are obtained.

3.4. Packing of Tcm A2 oxygenase molecules in the crystal

The presence of two-, three- and sixfold non-crystallographic symmetry in the hexagonal space group supports the V_M calculation of six monomers per asymmetric unit. Analysis of the self-rotation functions of the hexagonal crystals produces two potential configurations of Tcm A2 oxygenase monomers packing in the asymmetric unit: a dimer of trimers or a half a dimer of hexamers. In the first case, the non-crystallographic threefold axis of the trimer would be parallel to the crystallographic twofolds. This arrangement of the monomers will produce twofolds emanating perpendicular to the threefold every 60°, as observed in Fig. 1(*c*). The trimer threefold and crystallographic twofold compound to form the non-crystallographic sixfolds observed. The superposition of the dimers of trimers in reciprocal space will produce the appearance of a hexamer and hence three additional non-crystallographic twofolds.

Further consideration could not rule out each asymmetric unit containing a dimer of hexamers. In this case, each asymmetric unit would contain half of each of the two hexamers. A twofold relating the asymmetric units would relate these two halves to complete the dimer of hexamers. A crystallographic twofold axis would then be parallel to the non-crystallographic sixfold axis. This would produce the non-crystallographic symmetry observed, three sixfold axes, associated threefolds and twofold axes every 30° perpendicular to the sixfolds. However, this packing is unlikely given the conclusive D_3 symmetry seen in the tetragonal crystal form.

3.5. Conclusions

Observing the large number of monomers in the asymmetric of both of these crystal forms was unexpected because original native gels and size-exclusion chromatography implied the enzyme exists in a monomeric form. However, in light of the crystal packing results, a native gel run on crystals dissolved in diluted mother liquor showed evidence of oligomerization up to hexamers (not shown). Whether oligomerization has significance to the function or mechanism of the enzyme or is concentration dependent remains to be seen. In the future, the structure of this enzyme will shed light on the complex nature of the Tcm A2 oxygenase and its unique triple hydroxylation reaction and possible multimeric significance.

JB is supported from the Public Health Service/NIH training grant T32GM07377. BS thanks the donors of the Petroleum Research Fund administered by the American Chemical Society and the Searle Scholars Program/The Chicago Community trust for partial support of this work. Some of the work reported here was performed at SRRL, which is operated by the Department of Energy, Office of Basic Energy Sciences. The SSRL Biotechnology Program is supported by the National Institutes of Health, National Center for Research Resources, Biomedical Technology Program and by the Department of Energy, Office of Biological and Environmental Research.

References

Collaborative Computational Project, Number 4 (1994). *Acta Cryst.* D**50**, 760–763.
Decker, H., Motamedi, H. & Hutchinson, C. R. (1993). *J. Bacteriol.* **175**, 3876–3886.
Dowd, P., Hershline, R., Ham, S. W. & Naganathan, S. (1994). *Nat. Prod. Rep.* **11**, 251–264.
Egert, E., Noltemeyer, M., Siebers, J., Rohr, J. & Zeeck, A. (1992). *J. Antibiot.* **45**, 1190–1192.
Enroth, C., Neujahr, H., Schneider, G. & Lindqvist, Y. (1998). *Structure*, **6**, 605–617.
French, G. S. & Wilson, K. S. (1978). *Acta Cryst.* A**34**, 517–525.
Gould, S. J., Kirchmeier, M. J. & Lafever, R. E. (1996). *J. Am. Chem. Soc.* **118**, 7663–7666.
Hope, H. (1990). *Annu. Rev. Biophys. Biophys. Chem.* **19**, 107–126.

McPherson, A. (1976). *Methods of Biochemical Analysis*, Vol. 23, edited by D. Glich, pp. 249–345. New York: John Wiley.
Matthews, B. W. (1968). *J. Mol. Biol.* **33**, 491.
Otwinowski, Z. & Minor, W. (1997). *Methods Enzymol.* **276**, 307–326.
Schreuder, H. A., Laan, J. M. van der, Hol, W. G. & Drenth, J. (1988). *J. Mol. Biol.* **199**, 637–648.
Shen, B. & Hutchinson, C. R. (1994). *J. Biol. Chem.* **269**, 30726–30733.
Tong, L. & Rossmann, M. G. (1990). *Acta Cryst.* A**46**, 783–792.
Udvarnoki, G., Wagner, C., Machinek, R. & Rohr, J. (1995). *Angew. Chem. Int. Ed. Engl.* **34**, 565–567.
Weber, W., Zahner, H., Seibers, J., Schroder, K. & Zeeck, A. (1979). *Arch. Microbiol.* **121**, 111–116.